Reports on Geodesy and Geoinformatics, 2018, Vol. 105, pp. 19–28

DOI: 10.2478/rgg-2018-0003
Received: 13 October 2017 / Accepted: 30 January 2018
Published online: 30 June 2018

ORIGINAL ARTICLE

Measurement point density and measurement methods in determining the geometric imperfections of shell surfaces

Rafał Kocierz[1*], Michał Rębisz[2] and Łukasz Ortyl[1]

[1]Department of Engineering Surveying and Civil Engineering, Faculty of Mining Surveying and Environmental Engineering, AGH University of Science and Technology, 30 Mickiewicza Av, 30-059 Krakow, Poland
[2]Faculty of Physics and Applied Computer Science, AGH University of Science and Technology, 30 Mickiewicza Av, 30-059 Krakow, Poland

*kocierz@agh.edu.pl

Abstract

In geodetic measurements of deformations in shell cooling towers, an important factor is to optimize the number of points representing the exterior surface of the shell. The conducted analyses of damage to such structures proved that cooling towers exhibited shell deformation consisting of irregular vertical waves (three concavities and two convexities), as well as seven horizontal waves. On this basis, it is claimed that, in accordance with the Shannon theorem, the correct representation of the generated waves requires the measurement of the cooling tower shell in a minimum of 12 vertical and 14 horizontal sections. Such density of the points may not be sufficient to represent local imperfections of the shell. The article presents the results of test measurements and their analysis, which were conducted to verify the assumptions as to the optimal number of measurement points for the shell of a cooling tower. The evaluation was based on a comparative analysis of the data obtained by the Terrestrial Laser Scanning (TLS) method, creating a very detailed model of geometric imperfections in an actual cooling tower with a height of 100 m. Based on the data obtained by the TLS method, point grids of various density were generated. An additional measurement of the cooling tower shell deformation was performed using a precise electronic total station with reflectorless measurement option. Therefore, it was possible to assess the accuracy of measurements by laser scanning in relation to measurements obtained by reflectorless total stations.

Key words: cooling towers, geometrical imperfection, minimal point density, deformation

1 Introduction

In thin-walled shell structures (such as cooling towers), the most important parameter is the correct shape. With appropriate curvature of these objects, a membrane state of stress occurs (momentless shells), which means that there are no tensile forces (Hill et al., 1990). By means of this property, shell walls can be much thinner than those of conventional buildings (the thickness of a hyperboloid shell at its thinnest point can reach 14 cm). Unfortunately, performance errors (both in construction and surveying) during construction, as well as the aging of a structure (cement leaching and corrosion of steel) contribute to the formation of geometric imperfections. Deviations from the designed shape significantly influence the state of stress in the structure, which in turn may lead to a construction disaster. The development of a reliable, accurate and economical method of measuring shell structures is currently becoming quite significant, as higher and higher structures are being constructed, with heights often reaching up to 200 m (Busch et al., 2002).

Using appropriate measurement and calculation techniques, it is possible to determine geometric imperfections in relation

This work is available in Open Access model and licensed under a Creative Commons Attribution-NonCommercial-NoDerivatives 4.0 License.
Publisher: De Gruyter

to both the theoretical model and the model best fitted to the factual circumstances. Due to the specific nature of the structure and the way of conducting further structural analysis with the performance of the finite element method, the results of deformation measurements should be presented in a manner relating to the surface, not the point. Therefore, for the measurement carried out in a discrete way to faithfully reflect the shape of the structure, it is necessary to perform it with an appropriate density. The first comprehensive works leading to determining the minimum number of vertical and horizontal sections of measurement points (Gigiel, 1993) were based on assessing the nature of typical deformations in the hyperboloid shells of cooling towers. Analysis of the cases of stability loss caused by dead load and wind load showed that, in most cases, in the vertical section, there are three irregular concavities and two convexities. Similarly, for the horizontal section, deformations of seven regular waves dominate. Using the Shannon theorem (Smith, 1999) on the sampling of a continuous signal of a limited spectrum, the minimum number of measurement points allowing the representation of geometric imperfections in a structure shell can be determined. Accordingly, in the vertical direction, the minimum number of measurement points should be 12, and in the horizontal direction, 14 points should be subject to measurement. This gives at least 168 points on the entire shell. According to the authors, such an analysis is approximate (based on the analysis of cooling chimneys which underwent damage) and may not represent the nature of deformations in a satisfactory manner.

The starting point for the analysis of the density of points should be to determine the desired value of the mean error of stresses in the shell. Based on the analysis in (Gigiel, 1998), it is evident that, in terms of the stability analysis, the accuracy of identifying the actual deformations using selected interpolation method based on group of measurement points should not be worse than 10% of the shell thickness at the throat. Assuming that the measurements are performed with limited accuracy and they are arranged in a regular grid, it was determined that the maximum measurement error for the points of the shell should not exceed 5% of the shell thickness at its thinnest point.

On this basis, and having a very detailed numerical model of the physical shape of the shell, it is possible to perform simulations which allow conclusions to be drawn about the minimum number of horizontal and vertical sections of the structure. This will, be a result for a specific case but, at a certain level of probability, it can be generalized. If the minimum number of points is determined, it must be verified whether their spatial location is of great significance for the end result, which is the model of the shell's geometric imperfections. In the case of a correctly specified number of sections, the differences between the models generated from the sets of points that differ only in the position of the measurement points should not be greater than the admissible error. The yielded results are of great importance when carrying out measurements of shells using the polar methods, and with the use of scanning reflectorless total stations, which do not perform measurements in a grid as dense as in the case of laser scanners.

The selection of a measurement method is as important as the grid density. For the measurement of shell structures, the most commonly used methods include the photogrammetric method (Chisholm, 1977), the method of ambient tangents (Jasińska and Preweda, 2004), spatial intersection (Ding et al., 1996; Shortis and Fraser, 1991), or the polar 3D method, prevalent in the era of total stations with a possibility of reflectorless measurements (Woźniak and Woźniak, 2011; Woźniak, 2008). Currently, a large development of laser scanning technology is observable, and it is useful in many areas. By means of its ability to spatially measure a large number of points in a short time, it appears to be an ideal technique for inventory measurements of the shape of shell structures (Ioannidis et al., 2006; Camp et al., 2013; Lancon and Piot, 2012). However, in light of the previously discussed requirements, the measurement accuracy should be taken into consideration. This is essential due to the fact that manufacturers of laser scanners usually fail to provide a complete accuracy characterization of their products. Therefore, it is not possible to make an a'priori accuracy analysis. That is why it is necessary to compare the results of the measurements performed with a laser scanner with the values of imperfections determined based on the measurements carried out using reliable measurement techniques.

2 Determining imperfections

In order to determine the value of imperfections (local deformations of the shell), equations to the surface of the second order should be determined which, for most of the cooling towers, is a single-shell rotational hyperboloid. The general equation to the surface of the second order takes the following form (Zwillinger, 2002):

$$\begin{aligned} F(x,y,z) = & a_{11}x^2 + a_{22}y^2 + a_{33}z^2 + 2a_{12}xy + 2a_{23}yz + 2a_{13}zx \\ & + 2a_{14}x + 2a_{24}y + 2a_{34}z + a_{44} = 0 \end{aligned} \tag{1}$$

where x, y, z – coordinates of the shell surface points and $a_{11}, a_{22}, a_{33}, a_{12}, a_{23}, a_{13}, a_{14}, a_{24}, a_{34}, a_{44}$ – coefficients of the equation. While $a_{11}, a_{22}, a_{33}, a_{12}, a_{23}, a_{13}, a_{14}, a_{24}, a_{34}, a_{44} \in \mathbb{R}$ and $a_{ij} = a_{ji}$.

In addition, for the rotational hyperboloid representing cooling towers, it is assumed that $a_{11} = a_{22}$ and $a_{12} = 0$ and the equation to surface takes the following form:

$$\begin{aligned} G(x,y,z) = & A_{11}(x^2 + y^2) + A_{33}z^2 + 2A_{23}yz + 2A_{13}zx \\ & + 2A_{14}x + 2A_{24}y + 2A_{34}z + 1 = 0 \end{aligned} \tag{2}$$

where $A_{ij} = A_{ji} = \frac{a_{ij}}{a_{44}} = \frac{a_{ji}}{a_{44}}$.

Determining the rotational hyperboloid equation coefficients requires the knowledge of at least seven points measured on the surface of the cooling tower. The greater number of points i enables the approximation of the coefficients by the Gaussian least squares method (Ghilani and Wolf, 2006). Then, the approximation equation takes the following form:

$$\begin{aligned} v_i = & x_i^2 dA_{11} + y_i^2 dA_{22} + z_i^2 dA_{33} + 2x_i y_i dA_{12} + 2y_i z_i dA_{23} \\ & + 2z_i x_i dA_{13} + 2x_i dA_{14} + 2y_i dA_{42} + 2z_i dA_{43} + G_{0,i} \end{aligned} \tag{3}$$

where x_i, y_i, z_i – coordinates of the points measured on the shell surface and dA_{ij}^0 – differences to the values of the equation coefficients. The value:

$$\begin{aligned} G_{0,i} = & x_i^2 A_{11}^0 + y_i^2 A_{22}^0 + z_i^2 A_{33}^0 + 2x_i y_i A_{12}^0 + 2z_i y_i A_{23}^0 \\ & + 2x_i z_i A_{23}^0 + 2x_i A_{41}^0 + 2y_i A_{42}^0 + 2z_i A_{43}^0 + 1 \end{aligned} \tag{4}$$

where A_{ij}^0 – the approximate values of the equation coefficients determined for the seven random points measured on the shell surface. In this way, based on the entire set of points measured on the shell, the coefficients of the surface equation, representing the outer shell of the cooling tower, are approximated.

In order to determine the values of the shell deformation, the geometric distance of the points representing the measured surface should be determined, relative to the reference surface. The reference surface may be the model surface, generated based on the design data, or the surface approximated from the as-built measurements. Knowing the nature of the reference surface, the directions which are normal for this surface and which pass through the measured points are calculated. The coordinates of the theoretical points on the approximated surface are determined from the following relationships:

$$\begin{aligned} x &= x_i + t_i N_{x_i}, \\ y &= y_i + t_i N_{y_i}, \\ z &= z_i + t_i N_{z_i}, \end{aligned} \tag{5}$$

where t_i – the unknown parameter, individual for each point and $N_{x_i}, N_{y_i}, N_{z_i}$ – components of the normal vector. The value of the parameter t_i is determined by substitution of the variables x, y, z to the equation approximating the surface:

$$\begin{aligned} & t_i^2 \left[A_{11}\left(N_{x_i}^2 + N_{y_i}^2\right) + A_{33}N_{z_i}^2 + 2\left(A_{13}N_{x_i}N_{z_i} + A_{23}N_{y_i}N_{z_i}\right)\right] \\ & + t_i\left[N_{x_i}^2 + N_{y_i}^2 + N_{z_i}^2\right] + A_{11}\left(x_i^2 + y_i^2\right) + A_{33}z_i^2 + 2A_{13}x_iz_i \\ & + 2A_{23}y_iz_i + 2A_{14}x_i + 2A_{14}x_i + 2A_{24}y_i + 2A_{34}z_i + 1 = 0 \end{aligned} \tag{6}$$

where $N_{x_i} = \frac{\partial G}{\partial x}, N_{y_i} = \frac{\partial G}{\partial y}, N_{z_i} = \frac{\partial G}{\partial z}$.

The solution are two roots of the parameter t_i, where the correct root is the one of a smaller mode value. Based on the parameter determined there from and the components of the normal vector, local point deformation of the shell is calculated. The value of the deformation is calculated from the following relationship:

$$\delta_i = t_i\sqrt{N_{x_i}^2 + N_{y_i}^2 + N_{z_i}^2} \tag{7}$$

Values of the deformations for all the measured points of the shell obtained in this way enable the preparation of a graphical presentation of the distribution of cooling tower surface deformation relative to the reference surface. A convenient form of presentation is a generated contour map of imperfections in the azimuthal projection. An important issue in this area is the modelling of imperfections based on a discrete set of measurement points.

3 Accuracy required to describe the shape of a shell

Structures of various types require different accuracy to carry out as-built measurements. These differences result from the sensitivity of a structure to the stress derived from geometric imperfections. In the case of shell structures, it is important to analyse the ratio of the critical stress in the shell containing imperfections (σ_{exp}) to the critical stress in the ideal shell (σ_{exp}^0) (Gigiel, 1998). The conducted study shows that the decrease in the stress parameter ($\sigma_{exp}/\sigma_{exp}^0$) occurs at axisymmetric and sinusoidal imperfections covering the entire shell. At the same time, the amplitude values of these imperfections are comparable to the thickness of the shell t_0. On this basis, from the point of view of the stability analysis, it may be concluded that the expected accuracy of a model describing the shape of a shell should not be worse than

$$\varepsilon = \frac{1}{10} \cdot t_0 \tag{8}$$

where t_0 – shell thickness at the throat of a hyperbole and ε – maximum permissible error of the model.

Assuming a normal distribution of errors and the confidence level of 95%, a permissible mean error of the model is given by the formula:

$$\sigma_{model} = \frac{1}{20} \cdot t_0. \tag{9}$$

The error of the model is affected by the method of its creation (the choice of the approximating or interpolating function), as well as the precision of the imperfection measurements. Assuming a uniform distribution of the measuring grid, the formula for the maximum error of the measurement method w_{meas}^{max} can be expressed as follows:

$$w_{meas}^{max} = \frac{\varepsilon}{2} \tag{10}$$

The value of w_{meas}^{max} should be identified with the limiting error of determining imperfections. In order to determine the permissible mean error of the measurement σ_{meas}, the 5% significance level was adopted, based on which the following relationship was obtained:

$$\sigma_{meas} = \frac{\varepsilon}{4} \tag{11}$$

4 Characteristics of the structure and methods of data capture

The structure, for which the measurement was performed and the study was made, was a hyperboloid cooling tower. The flue gas stack was designed and built in the shape of a single-shell rotational hyperboloid. The base contains prefabricated reinforced concrete columns carrying the loads onto the foundations. This cooling tower uses an autonomous chilled water tank, which is not linked in any way to the columns or the foundations. The apparatus located inside the chimney has been divided into three levels: drift eliminator, hot water distribution and packing. The above-mentioned cooling modules were supported by a reinforced concrete post and beam system, which is an independent support structure. The geometric parameters of the cooling tower are as follows: the diameter of the bottom edge of the shell is 75.3 m, the diameter of the throat is 41.0 m, the diameter of the chimney outlet is 42.7 m, the height of the cooling tower is 99.8 m, the shell height is 93.0 m, and the height of the throat is 84.7 m. For this cooling tower, the design data was available, by means of which it was possible to generate a set of points and the 3D surface model of the cooling tower with the design parameters. The design thickness of the shell at the base was 0.54 m and decreased to 0.14 m at the shell height of 15 m. The value of 0.14 m continued until 89 m, where the thickness of the shell increased to 0.19 m at the top.

The measurements on this cooling tower were performed by two methods of surveying: a classical one, using a total station, and with a terrestrial laser scanner. The points representing the shell of the cooling tower in the classical measurement were obtained using a TCRP1201 total station. This instrument also performed the measurements of a control network and targets for the laser scanning in a local reference system. The accuracy parameters of this instrument are as follows: measurement to the prism: ±1 mm ± 1.5 mm, reflectorless measurement: ±2 mm ± 2 mm, measurement of direction ±0.0003 grads (Lambrou and Pantazis, 2010). Classical methods of surveying (tacheometric) were implemented by observing the shell of the cooling tower in 20 vertical and horizontal point strips through a commonly used 3D polar method (reflectorless distance measurement). A total of 400 points were obtained. The interval between subsequent vertical sections was approximately 4.9 m. The interval between subsequent hor-

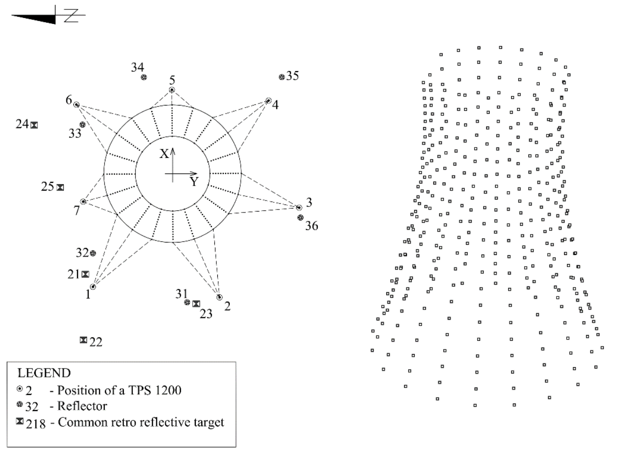

Figure 1. View of the measuring network and spatial distribution of the points measured by the 3D polar method

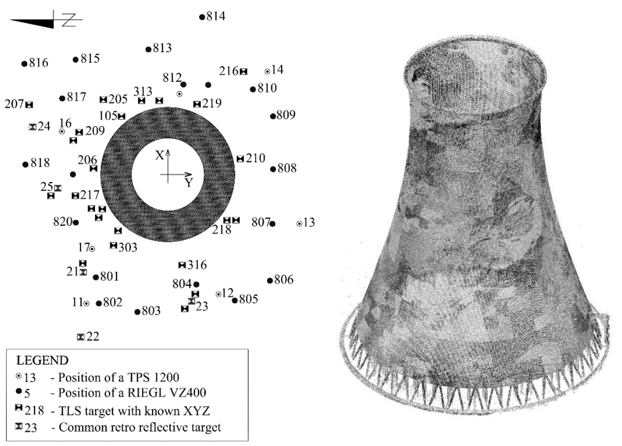

Figure 2. View of the scanning measurement network and the points on the cooling tower shell measured by the scanner

izontal strips was expressed in angular measure and equaled 20 grads (at the lowest point, the interval in the radian measure was 11.9 m). The control measurement established in the local coordinate system consisted of 18 points; 6 on tripods, 5 reflective tapes, and 7 free stations, from which 3 sections of the cooling tower were carried out for each one of them. The mean position error of the control points, after adjustment by the least squares method, did not exceed ± 1 mm horizontally and ± 2 mm for height. Figure 1 presents the distribution of the measurement control points and of the points measured on the cooling tower shell by the polar 3D method.

The point cloud representing the surface of the cooling tower was obtained using the Riegl VZ400 scanner. The accuracy of distance measurement for this scanner is given by the manufacturer as the degree of accuracy between the measured value and the true value, and is ± 5 mm to 100 m. Measurement precision is defined as the repeatability of performance and is estimated to be ± 3 mm. The measurement of the cooling tower using a terrestrial laser scanner was performed from 20 positions. The measuring mode which was used enabled the measurement of points with a density of 3 cm at a distance of 100 m. The 36 control points of the scanning control, black-and-white targets, were scanned with the basic scan density. Assuming an average distance of the scanner – scanning control point at 10 m, the density of scanning these points did not exceed 3 mm. Five points are retro-reflective targets, marked during the first measurement. These points enabled the combination of the two measurements. The remaining 31 points are seven positions of the total station and 24 black-and-white targets. The mean position error of the control points, horizontally and for height, did not exceed ± 2 mm. A combination of classical surveying and scanning results was carried out through the transformation of the scanning coordinates to the local reference system achieving an accuracy of ± 1 mm. Figure 2 presents the distribution of the control points and the point cloud of the cooling tower. Mutual fitting of the scans were performed in the Leica Cyclone program. They were implemented through reference points (17 black-and-white targets, 7 were not used) and clearly identifiable field points (27). A total of 213 homologous pairs of points were created, combining 20 scans. In addition to the Vertex Vertex combinations, Cloud-to-Cloud ones were also added. The resulting point cloud was obtained with an average error of scan record at the level of ± 3 mm, wherein the connection to the scanning network points did not have an error greater than ± 2 mm. The final cloud comprised 350 million points. In this form it was subjected to unification (without any reduction), and then exported. In Geomagic, it was subjected to the manual removal of the cooling tower infrastructure which did not belong to the shell of the flue gas stack, and the removal of the outliers. The algorithm for the removal of outliers, used at this stage, was based on the idea of the nearest neighbor. In the next step, the density of the cloud was decreased to a resolution of 3 cm between the points. Finally, a 14.8 million point cloud was obtained, representing the shell of the observed cooling tower.

It should be noted that the data was captured in actual field conditions, where it was not always possible to select the optimum position of the instruments relative to the structure. In the described analyses, an approximated surface was adopted as the reference surface on the basis of current measurements. Unfortunately, for this cooling tower there was no as-built measurement of the shell deformation, and the current measurements also showed a significant divergence from the design data.

5 Generating test samples of various density

The main objective of the conducted analysis was to determine the optimum density of the observed points grid on the test shell of the cooling tower, at which it was possible to define the effect (degree) of the shell deformation. A relationship was sought between reducing the number of observed points and the degree of quality degradation in the numerical model of imperfection. Based on a detailed and comprehensive numerical model, obtained with the technology of terrestrial laser scanning, a series of test samples were generated with a decreasing amount of observed points representing the surface of the cooling tower shell.

The process of generating test samples from the resulting cloud of points (14.8 million) was based on one of the basic geometric features of the observed object. A single-shell hyperboloid cooling tower has a vertical axis of symmetry (VAS), which was used as the basic construction line. Its location was determined as the geometric center of the observed structure for 14.8 million evenly distributed points on the outer shell of the chimney. The next stage comprised the development of a calculation scheme enabling the selection of individual groups of points from the global cloud. The designed calculation algorithm was implemented in the Python environment by creating a single program for the automatic selection of points. The selection was carried out based on the geometric parameters of the expected distribution grid of the points on the cooling tower shell, set by the operator. Due to the fact that the opera-

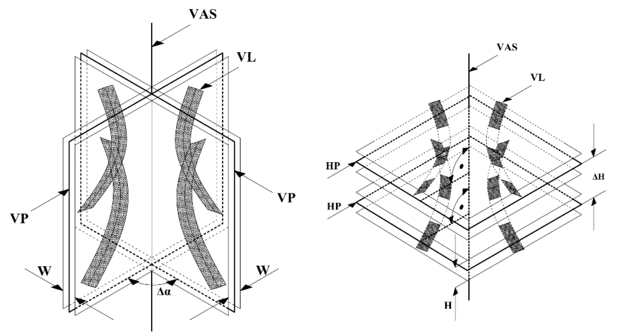

Figure 3. Graphical presentation of dependencies enabling the selection of the defined grid of points from the cloud

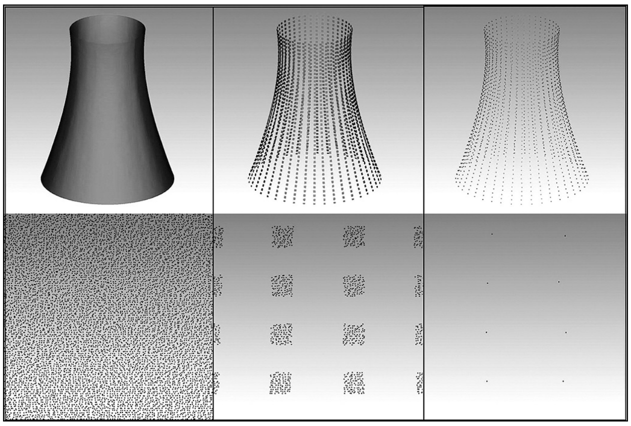

Figure 4. Graphical presentation of the selection of points from the cloud in the prepared program

tions were carried out for large data sets, the program activity was sequential. In the following calculation stage, the number of points taken for further selection was reduced. In the first step, a series of vertical planes (VP) was generated, going through the calculated axis of symmetry (VAS) (Fig. 3). Between the subsequent planes (VP), a horizontal angle interval ($\Delta\alpha$) was set. Then, the parameter W was defined, expressing the value of the width of the selected horizontal strips of the points (VL). In this way, a selection was made of the points (P) from the resulting cloud TLS, which fitted within the distance $\pm W/2$ relative to the vertical plane (VP). The next stage consisted of generating horizontal planes (HP). Only the strips of the cloud points included in the strips of the points VL were analyzed. All of the generated horizontal planes (HP) were perpendicular to the axis of symmetry (VAS). Between the subsequent planes (HP), a vertical distance interval (ΔH) was set. Then, the parameter H, expressing the value of the height of the selected horizontal strips of the points, was defined. For each subsequent plane, a selection of the points from VL was made, which fitted within the distance $\pm H/2$ relative to the horizontal plane HP. As a result, a grid of groups of points with the area dimension of WxH and the thickness in the radial direction, resulting from the properties of the captured point cloud, was obtained. In the last stage of the calculations, a single point representing the selected group of points of the cloud from the area WxH was determined. The problem was solved by using a median filter within a set group of points for the distance of VAS – P. Figure 4 graphically presents the effect of the selection of points.

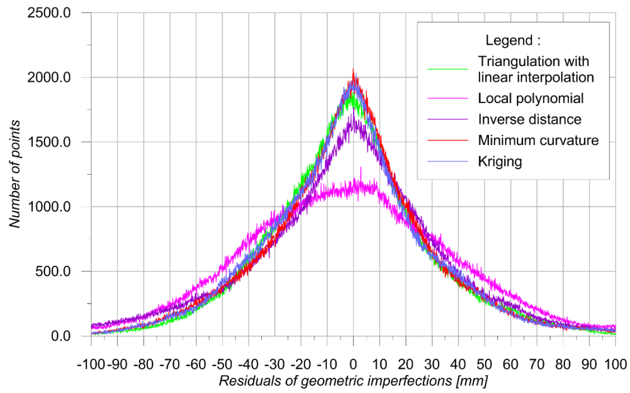

Figure 5. Histogram of differences in interpolation models with respect to the actual state

6 Selecting a method for modeling imperfections

It is essential to take into consideration the fact that the data obtained using the TLS technique and the polar method have the form of points. This property is of particular importance in the case of the observed shell structures, where special attention is paid to deformation processes. These phenomena, by definition, are characterized by a slow change in the dynamics of geometry and a relatively large local range. These features make the geometric imperfections which occur on the shell surface, seen as continuous deformations, discretized by single geodetic observations. In order to reflect the correct behaviour of the sampled spatial phenomenon, it seems extremely important to select a mathematical model interpolating the observed process. For the purposes of modelling shell deformation, simple models were used, such as the linear interpolation method (in the scope of a triangle grid), inverse distance and local polynomial, as well as more advanced methods, including the method of minimum curvature and Kriging (Davis, 2002; Li and Heap, 2011; Jin, 2008; Li and Heap, 2014; Isaaks and Srivastava, 1989).

Based on a dense set of points, with the distance between the points of 0.10 m, forming a regular grid of 1200 horizontal and 927 vertical sections, a test sample was created with a set of 400 selected points arranged in 20 horizontal and vertical strips. Based on the test sample (20x20) for each of the aforementioned modeling methods, a grid model has been created in the Surfer program by Golden Software, with the dimensions and distribution of the grid nodes consistent with the parameters of the grid of reference points (1200 columns and 927 rows). The basis for the assessment of individual modelling methods was the level of spatial discrepancies between the generated numerical model, and the actual shape of the shell (represented by 1,112,400 points in a grid of 1200 columns and 927 rows). This task was solved by using the residuals functions in the Surfer program. For each point of the reference set, a distance was studied with respect to the generated model. In the case of ideal behaviour of a given modelling method used, these distances should be equal to zero. For the overall assessment of the quality of the interpolated spatial model, summaries were prepared. The following chart presents a comparison of histograms presenting nodal point deviations of individual generated models with respect to the reference (original) point cloud (Fig. 5). All of the applied modelling methods showed a certain degree of discrepancy, mainly resulting from the low density of the set of points, based on which the modelling was performed. The essence of this comparison is not the value of the differences in imperfections, but the analysis of the differences between the models. Comparing the histograms, it can

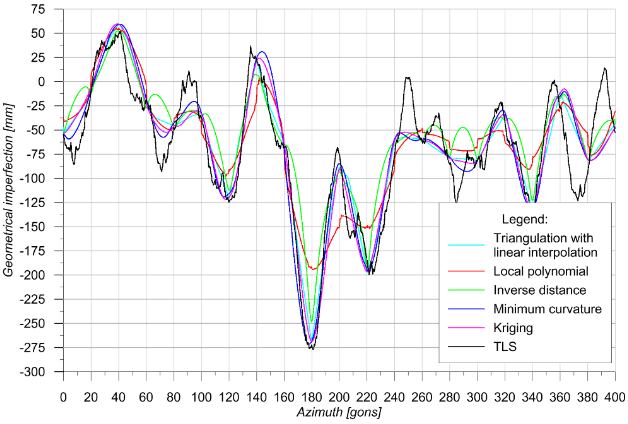

Figure 6. Horizontal section of interpolation models of shell deformation at a height of 45.00 m

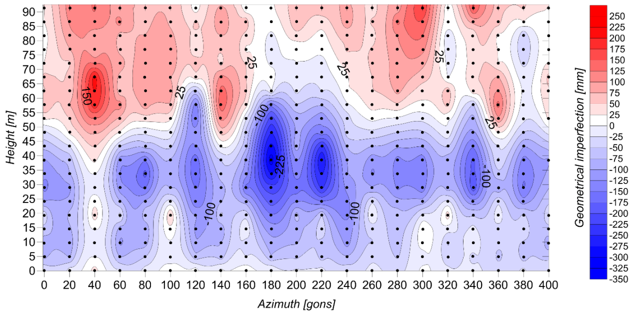

Figure 7. The map of the distribution of geometric imperfections for the No. 8 sample

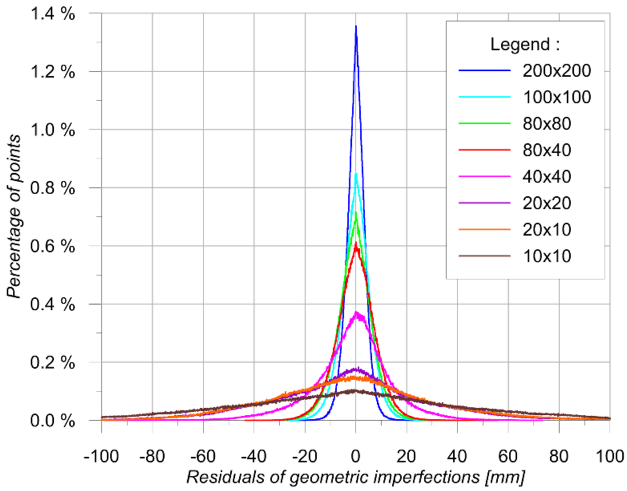

Figure 8. Histogram of the differences between the models

be noticed that the models created using local polynomial and inverse distance functions showed the lowest compliance with the real model. In order to more precisely verify the nature of the occurring discrepancies, three transverse horizontal sections were generated at the heights of 25.00 m, 45.00 m and 65.00 m. Analysis of the section generated at the height of 45.00 m (Fig. 6) confirms that, except for the models for which the deformations of the grid nodes were interpolated by the local polynomial and the inverse distance methods, the applied modelling methods allowed the nature of the shell deformation to be precisely reflected. Analysis of the created models also shows that the maximum deviation of the created models, relative to the existing state, occurs in the middle of the section joining the points that were used to build the model (for the test sample with a set of 400 selected points maximum differences reached 100 mm at 3sigma level for all of the modelling methods besides local polynomial). The value of the discrepancies depends on the model used, as well as on the density of the points used for interpolation.

In order to select the best method for modelling the geometric imperfections of cooling tower shells, both histograms of the differences in imperfections, as well as the created horizontal sections, were used. For the purposes of further analyses, the authors of this paper decided to select the Kriging method as the optimal method of modelling the observed phenomena. This choice was dictated by the smallest degree of deviation of the generated model relative to the actual surface.

7 Analyzing the effect of the point density on the accuracy of the shell shape deviation model

Based on the scanning results for further comparisons, a set of points was selected distributed evenly in the horizontal section at 0.3333 g (0.3°), and in the vertical section at 0.100 m. The selected horizontal interval corresponds to the length of the arc of the shell at the throat, amounting to 0.107 m. In the final result, the set of reference points consists of a grid with the dimensions of 1200 columns and 927 rows. According to the algorithm presented in the chapter "Generating test samples of various density" (5), the density of the reference set was decreased so that the distances between the points were a multiple of the basic interval, thus forming test sets, whose parameters have been summarized in the following table (Tab. 1).

In order to verify if the projection of the shell deformation was true, the density of the samples with enlarged intervals (Nos. 2-10) was increased to 1200 columns and 927 rows by interpolation, using a geostatistical function – Kriging. In order to determine the parameters of the interpolation function and to calculate geometric imperfections of the shell for nodal points of the grid, the Golden Software Surfer program was used. Figure 7 presents an example visualization of the grid with increased density and dimensions 20x20. For each of the models generated in this way, differences with respect to the reference model were calculated (sample 1). The designated residuals were analysed statistically and the results were presented in a tabular form (Tab. 2) and in the form of a histogram (Fig. 8).

It can be noticed that, with the reduction in the density of the test samples, the level of discrepancies of the created models relative to the actual surface increases. This is due to a large number of local deformations in the shell shape which can not be correctly imaged using a small number of points. A particularly high level of generalization (simplification) of the model of the shell's geometric imperfections is visible in the samples for which the number of horizontal sections is fewer than 80. This is very important because, for the models with a greater or equal number of columns, the mean deviation of the model difference does not change in a significant way. It was also observed that the predominant role in the proper projection of the model of the studied shell deformation is played by the number of horizontal sections, rather than by vertical ones. This thesis is confirmed by the results of the analyses of the following sets of measurements: 80x80, 80x40, 20x20 and 20x10. Comparing the pairs of sets with the same number of columns (80 and 20, respectively), slight changes in descriptive statistics can be observed, and their graphic representation is possible in the form of a histogram. Despite the use of the modular slab formwork,

Table 1. Characteristics of the test data

No.	No. of cols	No. of rows	No. of points	Interval between points in the horizontal plane angular [gons]	shell bottom [m]	shell throat [m]	shell top [m]	Interval in the vertical plane [m]
1	1200	927	1112400	0.3333	0.197	0.107	0.112	0.100
2	200	200	40000	2.0000	1.183	0.644	0.671	0.500
3	100	100	10000	4.0000	2.366	1.288	1.341	0.900
4	80	80	6400	5.0000	2.957	1.610	1.677	1.200
5	80	40	3200	5.0000	2.957	1.610	1.677	2.300
6	40	80	3200	10.0000	5.914	3.220	3.354	1.200
7	40	40	1600	10.0000	5.914	3.220	3.354	2.300
8	20	20	400	20.0000	11.828	6.440	6.707	5.000
9	20	10	200	20.0000	11.828	6.440	6.707	10.000
10	10	10	100	40.0000	23.656	12.881	13.415	10.000

Table 2. Descriptive statistics of the differences in imperfections of the models with the density decreased relative to the reference model

No. of the original sample	2	3	4	5	6	7	8	9	10
Dimension of the original grid	200x200	100x100	80x80	80x40	40x80	40x40	20x20	20x10	10x10
Avg distance [mm]	0.0	0.0	-0.6	-0.1	-2.8	-1.6	-2.3	-1.6	-4.3
Avg absolute distance [mm]	2.8	4.4	5.3	5.9	10.9	11.2	24.2	25.7	40.7
STD of distance [mm]	3.7	5.7	6.9	7.6	15.0	15.4	32.1	33.6	54.6
STD of absolute distance [mm]	2.4	3.7	4.5	4.9	10.7	10.7	21.2	21.8	36.6
Median [mm]	0.0	0.1	-0.4	0.0	-1.8	-0.6	-2.1	-2.2	-3.0
Min. [mm]	-27.6	-37.2	-41.4	-43.6	-103.2	-101.7	-149.4	-153.2	-244.8
Max. [mm]	40.4	44.7	54.6	55.9	79.7	73.4	149.4	168.2	244.8
Dispersion[mm]	68.0	82.0	96.0	99.5	182.9	175.1	298.8	321.4	489.6
Lower quartile [mm]	-2.2	-3.5	-4.7	-4.8	-10.1	-9.3	-21.3	-22.5	-34.8
Upper quartile [mm]	2.2	3.4	3.7	4.7	5.2	7.0	15.2	17.3	26.7

STD – standard deviation

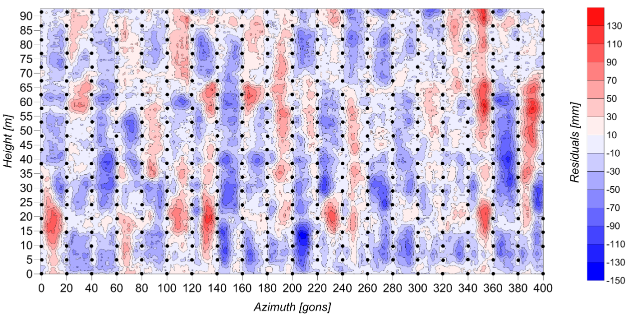

Figure 9. Map of the residuals for Model No. 8 (size 20x20) with respect to the reference model

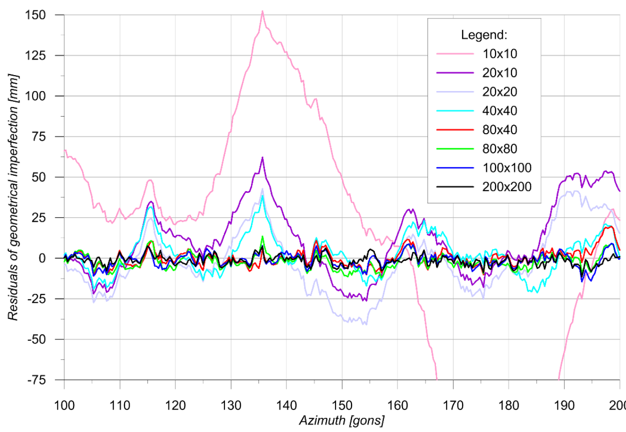

Figure 10. A fragment of the graph of the differences in geometric imperfections of the individual models at the height of 45 m

the conformity of maintaining the shape in the vertical plane is much higher than in the horizontal section. For the purpose of interpreting the obtained results more easily, differential models of successive sets of data (models 2–10) were also prepared, with respect to the reference set. A model of the differences for Model No. 8 (the original size of 20x20) is presented in Figure 9. For each model of deviations, three horizontal sections intersecting the shell at the height of 25.00 m, 45.00 m and 65.00 m were performed. Figure 10 contains a fragment of the graph of the differences in geometric imperfections of the individual models at the height of 45.00 m.

Based on the generated maps of differences in imperfections (Fig. 9), as well as horizontal sections (Fig. 10), it can be confirmed that the analysed shell has a large number of high frequency waves. Detailed analysis of the maps of differences in generated models with respect to the actual surface shows that they occur, in particular, in the horizontal sections.

Table 3. Descriptive statistics of differences in model imperfections, depending on the density of the grid and spatial distribution of the points on the cooling tower shell

Data set	40x40				80x40				80x80			
Turn φ [grad]	0	2.5	5	7.5	0	1.25	2.5	3.75	0	1.25	2.5	3.75
Avg distance [mm]	-1.6	0.5	2.2	0.0	-0.1	-0.1	0.1	-0.4	-0.6	-0.6	-0.4	-0.8
Avg abs. distance [mm]	11.2	10.5	10.3	10.9	5.9	6.0	5.9	5.9	5.3	5.3	5.3	5.2
STD of distance [mm]	15.4	14.0	13.5	14.8	7.6	7.7	7.6	7.6	6.9	7.0	6.9	6.8
STD of abs. distance [mm]	10.7	9.3	9.0	10.0	4.9	4.9	4.8	4.8	4.5	4.5	4.5	4.4
Median [mm]	-0.6	0.5	1.8	0.1	0.0	0.0	0.2	-0.2	-0.4	-0.4	-0.3	-0.6
Min. [mm]	-101.7	-76.1	-78.5	-83.6	-43.6	-47.1	-48.6	-41.6	-41.4	-45.7	-45.5	-42.1
Max. [mm]	73.4	73.9	80.7	85.6	55.9	47.6	55.1	61.6	54.6	50.1	51.5	64.8
Dispersion [mm]	175.1	150.0	159.2	169.2	99.5	94.7	103.7	103.2	96.0	95.8	97.0	106.9
Lower quartile [mm]	-9.3	-7.5	-5.8	-7.9	-4.8	-4.9	-4.6	-5.1	-4.7	-4.7	-4.5	-4.8
Upper quartile [mm]	7.0	8.4	9.8	8.1	4.7	4.7	5.0	4.4	3.7	3.7	3.8	3.4

STD – standard deviation

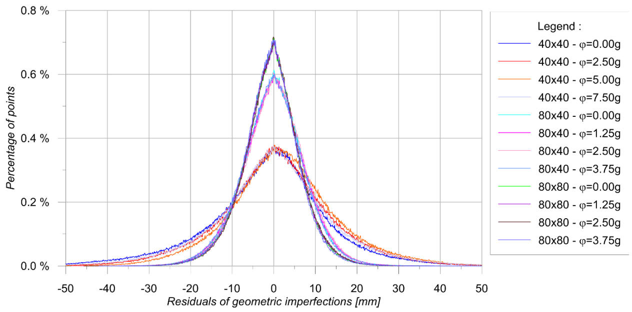

Figure 11. Histogram of differences between models depending on the grid density and spatial distribution of the points

8 Assessing the effect of the measuring grid distribution on the imperfection model

Another analysis of the measurement material was performed in order to obtain information concerning whether the spatial distribution of a grid of points with the same density, observed on the studied shell of the cooling tower, significantly affects the value of the determined model of imperfection. This task was carried out by comparing the differences in the values of imperfection for the test samples with the same geometric characteristics (grid density) but variable spatial distribution of the points on the shell.

Three reference grid densities were selected: 80x80, 80x40 and 40x40. These grids were of particular interest as they could be a sought optimum in surveying. With respect to the analysed grid of points, additional selections of the sets of points were made. The differentiating factor for the selected sets of points in a given grid was their spatial position on the observed structure. During the selection process, for successive sets of points, the selection algorithm was turned around the vertical axis of symmetry of the analysed structure. The step of φ was as follows: $\Delta\alpha/4$, where $\Delta\alpha$ was the interval in the angular measure between the measuring horizontal of the reference set of points. In this way, three groups of test samples were obtained. Each of them consisted of four sets of points with identical geometric properties, but with different positions. The new sets of points, just as the reference sets, were subjected to an analogous calculation scheme. In particular, the value of the spatial discrepancy between the model obtained for the reference set (1200 x 927) and the model based on the analysed test sample were studied. For this purpose, statistical parameters were calculated, describing the observed phenomena as well as the histograms of deviations of the test model with respect to the reference model. The histogram in Figure 11 and the summary Table 3 present the results obtained for all the analysed sets of points.

For the 80x80 group, the maximum mutual differentiation between the determined standard deviations did not exceed 0.2 mm. A similar scale of deviations was demonstrated by other statistical parameters calculated for this group of points. The histograms of distance of the reference set, relative to successively obtained models of test samples, coincided throughout the whole observed range. The calculation results obtained for the set of points of the remaining grid densities (80x40 and 40x40) demonstrated coherence with the results obtained for the 80x80 group. In addition, it was noticeable that, with the decreasing density of the point grid, the mutual differentiation of the results increased. This could be seen on the example of standard deviation modes. In the case of the 80x80 and 80x40 point grids, the maximum mutual differences of this parameter were 0.1 mm. In contrast, for the 40x40 grid, the mutual differences increased to 1.7 mm. Based on the obtained results, it can be seen that within each of the three groups of point grids, there are small mutual differentiations of the main statistical parameters, as well as a slight deviation of the distance histograms. This may prove the similar behaviour of the generated deformation models based on the test samples with identical geometric properties but with a different position. These conclusions confirm the lack of randomness in the results obtained for the reference sets of points. There are reasonable grounds to believe that, for the analysed measurement structure, the use of a measuring grid with the geometric properties which are such as in the discussed research samples, will allow correct results to be obtained regardless of the spatial distribution of the grid points on the cooling tower shell.

9 Comparing the method of terrestrial laser scanning and the 3D polar measurement

In order to verify the suitability of the terrestrial laser scanning method for the purpose of conducting measurements of shell structure deformations, the precision of the obtained geometric imperfections should be evaluated. In the case of measuring a dense point cloud, the modelling errors should be considered negligible, and the permissible mean error of determining imperfections is expressed by the formula (9). If, as a result of the measurement, a cloud of low density is generated, requiring a further increase of its density in the subsequent step, the permissible mean error of determining deformation is expressed by the formula (11). In the case of the discussed cooling tower, whose thickness of the thinnest part is 140 mm, the above mean errors amount to ± 7 mm and ± 3.5 mm.

By means of the fact that the performed scanning measure-

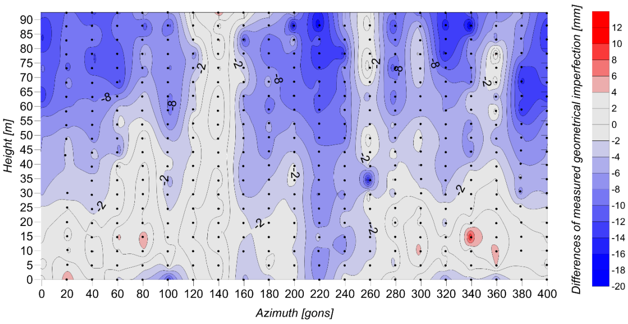

Figure 12. Map of imperfection differences determined by the polar method and TLS

Table 4. Descriptive statistics of the set of differences in imperfections between the polar and the scanning measurement

Statistics	Value [mm]
Mean difference of imperfection	-3.9
STD of imperfection differences	4.7
Median	-3.4
Min.	-18.8
Max.	10.1
Dispersion	28.9
Lower quartile	-7.2
Upper quartile	-0.5

STD – standard deviation

ments were tied to the coordinate system of the total station measurement, it was possible to compare the determined deformations for both of these measurements. For each point determined in the reflectorless manner (measured in the 20x20 grid) a corresponding point in the point cloud was found, and the value of the geometric imperfection of the shell shape was calculated for both of them. A statistical description of the set of differences in imperfections determined by both measuring techniques is summarized in Table 4.

For the evaluation of the spatial distribution of the differences, their graphical presentation was also prepared, in the form of the development of the shell surface on the plane (Fig. 12). Based on the analysis of the map of imperfection differences (Fig. 12), it can be observed that the differences in measurement values between the method of laser scanning and the 3D polar method increase with the height of the shell. Up to a height of 50 m, the standard deviation is ±3.9 mm, while higher – it is ±8.1 mm. The obtained deviations are not considered to be noise, which excludes random measurement errors or errors associated with determining the orientation parameters of the scanner positions. Attention should be paid to the relatively small number of local interferences between the measurements (at the 2% level). They may be due to the local shell failures (e.g. stepwise performance errors that occur at the edges of modular slab formwork) or measurement errors (measurement noise). The accuracy and reliability of the polar measurement method was confirmed by measuring one section from two measurement stations, which was ±4 mm. In order to check the noise level for the laser scanning method, for each point determined by the classical surveying technique, the value of imperfection was calculated by the method of laser scanning in a different way. Namely, it was determined as the average of all the cloud points located at a distance of 0.100 m and 0.200 m from the point measured with the reflectorless total station. Table 5 presents descriptive statistics for comparing these generated models. When comparing the determined imperfection deviations with the results shown in Table 4, a

Table 5. Comparing the polar method with the laser scanning method (averaging the points)

Statistics	Imperfections of laser scanning determined as the arithmetic mean of a set of points	
	In the range of 0.100 m	In the range of 0.200 m
Avg number of averaged points	28	113
Mean diff.* of imperfection [mm]	-4.0	-4.0
STD of imperfection diff.* [mm]	4.6	4.8
Median [mm]	-3.6	-3.7
Min. [mm]	-16.8	-18.0
Max. [mm]	7.3	6.9
Dispersion [mm]	24.1	24.9
Lower quartile [mm]	-7.3	-7.4
Upper quartile [mm]	-0.4	-0.4

STD – standard deviation
*difference

slight change in the dispersion value of the imperfection differences (of about 4 mm) could be noted, as well as a constant value of standard deviation of the imperfection differences with respect to the polar method. This means that the used laser scanner is characterized by a low noise level, and the use of a low pass filter does not substantially improve the precise of the model.

Considering that the standard deviation of the imperfection differences determined in Table 4 and Table 5 results from the error in both performed measurements, the obtained values are much higher than the values resulting from the formula (11), based on which the mean error of measurement for this specific case should not exceed ±3.5 mm. It should be noted, however, that the experiment proved that a reasonable consistency between the two measurements was obtained for the lower part of the shell. Applied method of measurement, the laser scanner, and the post-processing algorithm of the scanner data, allow experts to obtain the necessary accuracy required while evaluating the technical condition of the tested shell.

10 Conclusions

Among the imperfection models generated by linear interpolation (in the scope of a triangle grid), inverse distance and local polynomial, as well as the minimum curvature method and Kriging, only the minimum curvature method and Kriging properly reflected the values of imperfection. Both methods showed a mutually comparable degree of discrepancies between the model and the actual shape of the shell.

Among the models generated from the point grids with decreased density, and the model discrepancies referred to the reference model (the 1200x927 grid), smaller than the permissible mean error occurred for the grids with the number of columns and rows at least equal to 80x80. Analyzing the descriptive statistics of the sets with the same number of columns (80 and 20, respectively), it was noted that the number of horizontal sections, rather than vertical ones, played the predominant role in the proper projection of the deformation model of the test shell.

For the measured point grids that meet the accuracy criterion imposed by the model (9), no significant changes were observed in the precision of modeling imperfections at different options of their distribution on the test structure (e.g. for the four 80x80 grids, standard deviations of the average mode of imperfection differ by 0.2 mm). Naturally, the grids with lower density, 40x40, exhibit a coherent relationship, but larger discrepancies in the values of descriptive statistics. There are reasonable grounds to believe that, for the analyzed measurement structure, the use of a measuring grid with the geometric properties such as the ones in the discussed research samples, will allow correct results to be obtained regardless of the spatial distribution of the grid points on the cooling tower shell.

A comparison of the imperfection values, determined in the discrete points measured by the polar method and the same ones selected from the TLS, demonstrates the compliance at the level of ±3.9 mm up to a height of 50 m; higher these values increase to ±8.1 and are not considered to be noise. This indicates the occurrence of the error of scale between the two methods, which occurs with sharp vertical angles. While subsequent measurements are performed with the same device, the scale error will not matter; the problem occurs with the change in the methods or measurement tools. The descriptive statistics obtained from the analysis demonstrated that it was insignificant whether the point selected from a cloud was single or averaged from the adjacent area (10x10 cm and 20x20 cm), which means that the used scanner has a low noise level.

When measuring with the laser scanning method, the resultant cloud is so dense that additional increasing of its density by modeling methods is not required. In this case, the permissible mean error of determining imperfections can be calculated from the formula (9), and for the structure in question it is ±7 mm. With this assumption, the obtained standard deviation values confirm the possibility of using the laser scanning method for measuring shell deformations of the hyperboloid cooling towers.

Acknowledgement

The research studies were carried out as part of the AGH statutory research number 11.11.150.005. The authors would like to express their gratitude to the company 3Deling, who provided the scanner for the measuring purposes, and to Bartosz Ajszpur, its representative, who participated in the implementation of the scanning surveys, as well as helping with his advice and experience in collecting the scanning material. We would also like to thank to Sławomir Naturalny and Michał Pańczyszyn, who significantly contributed to the capture of the measurement material.

References

Busch, D., Harte, R., Krätzig, W. B., and Montag, U. (2002). New natural draft cooling tower of 200 m of height. *Engineering Structures*, 24(12):1509–1521, doi:10.1016/S0141-0296(02)00082-2.

Camp, G., Carreaud, P., and Lançon, H. (2013). Large structures: which solutions for health monitoring? In *International Archives of the Photogrammetry, Remote Sensing and Spatial Information Sciences. XXIV ICIPA Symposium*, volume 5/W2, pages 137–141.

Chisholm, N. (1977). Photogrammetry for cooling tower shape surveys. *The Photogrammetric Record*, 9(50):173–191, doi:10.1111/j.1477-9730.1977.tb00080.x.

Davis, J. C. (2002). *Statistical and data analysis in geology*. John Wiley & Sons.

Gigiel, J. M. (1993). An approach to optimal space density of measurements of cooling tower shells. *Archives of Civil Engineering*, 2:179–191.

Ding, X., Coleman, R., and Rotter, J. M. (1996). Technique for precise measurement of large-scale silos and tanks. *Journal of Surveying Engineering*, 122(1):14–25, doi:10.1061/(ASCE)0733-9453(1996)122:1(14).

Ghilani, C. D. and Wolf, J. M. (2006). *Adjustment computations*. John Wiley & Sons.

Gigiel, J. M. (1998). *Synteza uwarunkowań konstrukcyjno-wytrzymałościowo-reologicznych dla pomiarowej rejestracji stanu chłodni kominowej (Synthesis of structural conditions, strength and rheological for measurement registration of cooling tower)*. Silesian University of Technology, Gliwice, Poland.

Hill, G. B., Pring, E. J., and Osborn, P. D. (1990). *Cooling towers: principles and practice*. Butterworth-Heinemann.

Ioannidis, C., Valani, A., Georgopoulos, A., and Tsiligiris, E. (2006). 3d model generation for deformation analysis using laser scanning data of a cooling tower. In *Proc. of 3rd IAG /12th FIG Symposium, International Federation of Surveyors, Baden*, volume 3, pages 22–24.

Isaaks, E. H. and Srivastava, M. R. (1989). *Applied geostatistics*. Oxford University Press New York.

Jasińska, E. and Preweda, E. (2004). A few comments on determining the shapes of hyperboloid cooling towers by the means of ambient tangents method. *Geodezja*, 10(1):19–29.

Jin, L. (2008). *A Review of Spatial Interpolation Methods for Environmental Scientists*. Department of Resources, Energy and Tourism, Geoscience Australia.

Lambrou, E. and Pantazis, G. (2010). Evaluation of the credibility of reflectorless distance measurement. *Journal of Surveying Engineering*, 136(4):165–171, doi:10.1061/(ASCE)SU.1943-5428.0000029.

Lancon, H. and Piot, S. (2012). New tools for the monitoring of cooling towers. In *Proc., 6th European Workshop on Structural Health Monitoring, German Society for Nondestructive Testing, Dresden, Germany*.

Li, J. and Heap, A. D. (2011). A review of comparative studies of spatial interpolation methods in environmental sciences: performance and impact factors. *Ecological Informatics*, 6(3-4):228–241, doi:10.1016/j.ecoinf.2010.12.003.

Li, J. and Heap, A. D. (2014). Spatial interpolation methods applied in the environmental sciences: A review. *Environmental Modelling & Software*, 53:173–189, doi:10.1016/j.envsoft.2013.12.008.

Shortis, M. R. and Fraser, C. S. (1991). Current trends in close-range optical 3d measurement for industrial and engineering applications. *Survey Review*, 31(242):188–200, doi:10.1179/sre.1991.31.242.188.

Smith, S. W. (1999). *The scientist and engineer's guide to digital signal processing*. California Technical Pub. San Diego.

Woźniak, M. (2008). Monitoring of construction shape changes using reflectorless techniques. *Reports on Geodesy*, 84(1):93–97.

Woźniak, M. and Woźniak, K. (2011). Geodetic measuring methods and shape estimation of concrete thin shell surface. *Reports on Geodesy*, 91(2):81–88.

Zwillinger, D. (2002). *CRC standard mathematical tables and formulae*. CRC press.